PHYSICAL REVIEW D **87,** 064042 (2013)

Charged-particle motion around a rotating non-Kerr black hole immersed in a uniform magnetic field

Ahmadjon A. Abdujabbarov,[1,2,3,*] Bobomurat J. Ahmedov,[1,2,3,†] and Nozima B. Jurayeva[1,4,‡]

[1]*Institute of Nuclear Physics, Ulughbek, Tashkent 100214, Uzbekistan*
[2]*Ulugh Beg Astronomical Institute, Astronomicheskaya 33, Tashkent 100052, Uzbekistan*
[3]*The Abdus Salam International Centre for Theoretical Physics, 34151 Trieste, Italy*
[4]*National University of Uzbekistan, Tashkent 100174, Uzbekistan*

(Received 20 November 2012; published 26 March 2013)

We present analytical solutions of Maxwell's equations around a rotating non-Kerr black hole immersed in an external uniform magnetic field. The influence of a magnetic field on the effective potential of the radial motion of a charged test particle around a rotating non-Kerr black hole immersed in an external magnetic field are investigated by using the Hamilton-Jacobi equation of motion. The dependence of the minimal radius of the circular orbits $r_{\rm mc}$ and the radius of the innermost stable circular orbits (ISCOs) from the deformation and the magnetic parameters for the motion of charged particles around a rotating non-Kerr black hole are also presented. An increase of the magnetic field decreases the ISCO radius, while the negative deformation parameter may lead to a larger ISCO radius. A comparison of the numerical results of ISCOs around a non-Kerr black hole with the observational data for the ISCO radius of rapidly rotating black holes [R. Shafee *et al.*, Astrophys. J. **636**, L113 (2006)] provides the upper limit for the deformation parameter as $\epsilon \leq 22$.

DOI: 10.1103/PhysRevD.87.064042 PACS numbers: 04.50.−h, 04.40.Dg, 97.60.Gb

I. INTRODUCTION

A rotating astrophysical black hole without an electric charge is uniquely described by the Kerr metric, which only possesses two parameters—the total mass M and the specific angular momentum a of the black hole—within four-dimensional general relativity according to the no-hair theorem [1–5]. However, in the regime of strong gravity, general relativity could break down, and astrophysical black holes might not be the Kerr black holes predicted by the no-hair theorem [6–8].

Recently, Johannsen and Psaltis proposed a deformed Kerr-like metric suitable for the strong field of the no-hair theorem, which describes a so-called rotating non-Kerr black hole [7]. The study of the particle orbits could provide an opportunity for constraining the allowed parameter space of solutions, as well as deeper insight into the physical nature and properties of the corresponding spacetime metrics. Therefore, in this work we study the electromagnetic field and charged particle motion around a rotating non-Kerr black hole immersed in an external magnetic field.

In a recent paper [9] the properties of the ergosphere and energy extraction by the Penrose process in a rotating non-Kerr black hole were investigated. The direct imaging of rapidly rotating non-Kerr black holes and their shadows were studied in Ref. [10]. Strong gravitational lensing by a rotating non-Kerr compact object was investigated in Ref. [11]. The strong dependence of the predicted energy spectra, the energy-dependent polarization degree, and the polarization direction on the parameters of a rotating non-Kerr black hole were found in Ref. [12]. A brief review of testing the Kerr black hole hypothesis was given in Ref. [13]. The accretion disc properties around a rotating non-Kerr compact object were considered in Ref. [14].

In principle, the properties of innermost stable circular orbits (ISCO) could provide a good tool for understanding the energetic processes of a black hole. The acceleration of particles, circular geodesics, the accretion disk, and high-energy collisions in the Janis-Newman-Winicour spacetime have been considered in Refs. [15,16]. Understanding the motion of test particles and particle acceleration mechanisms in an axial-symmetric spacetime may provide new tools for studying new important general relativistic effects, which are associated with nondiagonal components of the metric tensor and have no Newtonian analogues [17,18]. It has been recently shown in Ref. [19] that primordial Kerr superspinars—extremely compact objects with an exterior described by the Kerr naked singularity geometry—can serve as efficient accelerators for extremely high-energy collisions. The properties of the event horizon, the static limit for a charged rotating black hole solution of minimal supergravity theory, and particle motion have been considered in Ref. [20].

The paper is organized as follows. In Sec. II we look for exact solutions of the vacuum Maxwell's equations in the spacetime of a nonrotating black hole immersed in a uniform magnetic field. The equations of motion of charged particles and their motion at the equatorial plane in the vicinity of the rotating non-Kerr black hole are

*ahmadjon@astrin.uz
†ahmedov@astrin.uz
‡nozima@astrin.uz

considered in Sec. III. We obtain the effective potential for a charged test particle with a specific angular momentum, orbiting around the black hole, as a function of the external magnetic field, deformation parameter, and angular momentum of the non-Kerr black hole. In Sec. IV we find the exact expression for the dependence of the minimal radius of a circular orbit on the parameters of the spacetime metric around a rotating non-Kerr black hole. Some concluding remarks are given in Sec. V.

We use a system of units in which $c = G = 1$, a spacelike signature $(-, +, +, +)$, and a spherical coordinate system (t, r, θ, φ). Greek indices are taken to run from 0 to 3.

II. BLACK HOLE IMMERSED IN A UNIFORM MAGNETIC FIELD

The deformed Kerr-like metric that describes a stationary axisymmetric and asymptotically flat vacuum spacetime, in the standard Boyer-Lindquist coordinates, can be expressed as [7]

$$ds^2 = g_{00}dt^2 + g_{11}dr^2 + g_{22}d\theta^2 + g_{33}d\varphi^2 + 2g_{03}dtd\varphi, \tag{1}$$

with

$$g_{00} = -\left(1 - \frac{2Mr}{\Sigma^2}\right)(1 + h),$$
$$g_{11} = \frac{\Sigma^2(1 + h)}{\Delta + a^2 h \sin^2\theta}, \qquad g_{22} = \Sigma^2,$$
$$g_{33} = \sin^2\theta\left[\Sigma^2 + \frac{a^2(\Sigma^2 + 2Mr)\sin^2\theta}{\Sigma^2}(1 + h)\right],$$
$$g_{03} = -\frac{2aMr\sin^2\theta}{\Sigma^2}(1 + h),$$

where

$$\Sigma^2 = r^2 + a^2\cos^2\theta, \quad \Delta = r^2 - 2Mr + a^2, \quad h = \frac{\epsilon M^3 r}{\Sigma^4},$$

and the constant ϵ is the deformation parameter. The quantity $\epsilon > 0$ or $\epsilon < 0$ corresponds to the cases in which the compact object is more prolate or oblate than the Kerr black hole, respectively. As $\epsilon = 0$, the black hole is reduced to the typical Kerr black hole known in general relativity.

Here we will exploit the existence in this spacetime of a timelike Killing vector, $\xi^\alpha_{(t)} = \partial x^\alpha/\partial t$, and a spacelike one, $\xi^\alpha_{(\varphi)} = \partial x^\alpha/\partial\varphi$, which are responsible for the stationarity and axial symmetry of the geometry, such that they satisfy the Killing equations

$$\xi_{\alpha;\beta} + \xi_{\beta;\alpha} = 0, \tag{2}$$

which—according to the Wald method [21]—allows one to write the solution of the vacuum Maxwell's equations $\Box A^\mu = 0$ for the vector potential A_μ of the electromagnetic field in the Lorentz gauge in the simple form

$$A^\alpha = C_1\xi^\alpha_{(t)} + C_2\xi^\alpha_{(\varphi)}. \tag{3}$$

The constant $C_2 = B/2$ where the gravitational source is immersed in the uniform magnetic field $\mathbf{B}$, which is parallel to its axis of rotation. The value of the remaining constant C_1 can be easily calculated from the asymptotic properties of the spacetime (1) at infinity. Indeed, in order to find the remaining constant one can use the electrical neutrality of the black hole, $4\pi Q = 0$, evaluating the integral through the spherical surface at the asymptotic infinity. Then one can easily get the value of the constant as $C_1 = aB$.

Thus the four-vector potential A_μ of the electromagnetic field will take the following form:

$$A_0 = -aB\frac{\Sigma^2 - 2Mr + Mr\sin^2\theta}{\Sigma^2}(1 + h),$$
$$A_1 = A_2 = 0,$$
$$A_3 = \frac{1}{2}B\sin^2\theta\left[\Sigma^2 + \frac{(2Mr + \Sigma^2)\sin^2\theta - 4Mr}{\Sigma^2}a^2(1 + h)\right]. \tag{4}$$

The orthonormal components of the electromagnetic fields measured by zero-angular-momentum observers (ZAMO) with four-velocity components

$$(u^\alpha)_{\mathrm{ZAMO}} \equiv \left(\sqrt{\frac{\mathcal{R}}{\Sigma^2(1 + h)(\Delta + a^2 h\sin^2\theta)}}, 0, 0, -\frac{2Mar\sqrt{1 + h}}{\sqrt{\Sigma^2(\Delta + a^2 h\sin^2\theta)\mathcal{R}}}\right), \tag{5}$$

$$(u_\alpha)_{\mathrm{ZAMO}} \equiv \left(\sqrt{\frac{\Sigma^2(1 + h)(\Delta + a^2 h\sin^2\theta)}{\mathcal{R}}}, 0, 0, 0\right) \tag{6}$$

are given by the expressions

$$E^{\hat{r}} = \frac{aBM}{256\sqrt{\mathcal{R}}\Sigma^6(1 + h)}\mathcal{P}_1, \tag{7}$$

$$E^{\hat{\theta}} = \frac{aBMr}{\Sigma^2\sqrt{(\Delta + a^2\sin^2\theta)\mathcal{R}}}\mathcal{P}_2, \tag{8}$$

$$B^{\hat{r}} = \frac{B\cos\theta}{\Sigma^4\sqrt{\mathcal{R}}}\mathcal{P}_3, \tag{9}$$

$$B^{\hat{\theta}} = \frac{B\sin\theta}{2\Sigma^8}\sqrt{\frac{\Delta + a^2 h\sin^2\theta}{\mathcal{R}}}\mathcal{P}_4, \tag{10}$$

where the following notations have been introduced:

$$\mathcal{R} = \Sigma^4 + a^2(1 + h)(2Mr + \Sigma^2)\sin^2\theta,$$

$$\mathcal{P}_1 = \frac{1}{Mr}\{a^4(h\cos 4\theta - 4 - h) - 8r^4 - 4a^2r[2(1+h)M + (3+h)r]$$
$$- 4a^2[a^2 + r\{-2(1+h)M + r - hr\}]\cos 2\theta\}\{3a^4h + 12r^3(M + 4hM - 2hr) - a^2r[7(1+2h)M + 8hr]$$
$$+ 4[a^4h + (1+4h)Mr^3 - 2a^2r(M + 2hM + hr)]\cos 2\theta + a^2[a^2h - (1+2h)Mr]\cos 4\theta\}$$
$$- 2(1+h)\{2a^6h + 64r^6 + 16a^2r^3[6(1+4h)M + (4-3h)r]$$
$$- 8a^4r[7(1+2h)M + (-3+h)r] + a^2[a^4h - 32a^2(2M + 4hM - r)r$$
$$+ 16r^3(2M + 8hM + 4r + 3hr)]\cos 2\theta - 2a^4[a^2h - 4r(-M - 2hM + r + hr)]\cos 4\theta - a^6h\cos 6\theta\}\sin^2\theta, \quad (11)$$

$$\mathcal{P}_2 = -2(1+h)\left\{\frac{\Delta}{2} + \frac{r^4 - a^4}{\Sigma^4}3hMr + \frac{h}{\Sigma^2}[a^4 + 2a^2r^2 + r^3(-4M + r)] - \frac{Mr}{\Sigma^8}\left[a^4 + \frac{\Delta + Mr}{Mr}h\Sigma^4 - r^4\right]\right\}\sin 2\theta$$
$$+ \frac{1}{16\Sigma^8}\mathcal{R}\left\{\left[5a^6 + 32a^2h\frac{2M - r}{M}\Sigma^4 + a^4\left(11r^2 - \frac{16h\Sigma^4}{Mr}\right) - 16(r^6 + hr^2\Sigma^4)\right]\sin 2\theta\right.$$
$$\left. + 4a^2\left[a^4 - 2r^4 + 2h\Sigma^4 + a^2\left(r^2 - \frac{2h\Sigma^4}{Mr}\right)\right]\sin 4\theta + a^4(a-r)(a+r)\sin 6\theta\right\}, \quad (12)$$

$$\mathcal{P}_3 = a^2\Sigma^2(4hr^2 + \Sigma^2(1-2h)) - 2a^4[M(r+3hr) - h\Sigma^2] + r[r\Sigma^2(2hr^2 + \Sigma^2(1-2h))$$
$$+ 2M(r^2 - \Sigma^2)(r^2(1+3h) + \Sigma^2(1-h))], \quad (13)$$

$$\mathcal{P}_4 = 2a^8r\cos^8\theta + 2\cos^6\theta(-2a^8M + 4a^6r^3 + a^8M\sin^2\theta)$$
$$- 2a^2r\cos^2\theta\left\{-4r^6 + a^2\left[-2Mr^3 + \frac{4hM\Sigma^4}{r}\right] + a^2Mr\left[r^2 + \frac{h\Sigma^4}{Mr}\right]\sin^2\theta\right\}$$
$$+ \cos^4\theta\left\{-4a^6Mr^2 + 12a^4r^5 + a^6M\left[2r^2 + \frac{h\Sigma^4}{Mr}\right]\sin^2\theta\right\}$$
$$+ r^3\left\{2\left[r^6 + 2a^2Mr^3 + \frac{42a^2Mh\Sigma^4}{r}\right] - a^2M\left[2r^3 + \frac{8M + 3r}{Mr}\Sigma^4h\right]\sin^2\theta\right\} + a^4hM\Sigma^4\sin^2 2\theta. \quad (14)$$

The electromagnetic field (7)–(10) depends on the angular momentum and the deformation parameter in complex way. Astrophysically, it is interesting to know the limiting cases of the expressions (7)–(10); for example, in either the linear or quadratic approximation $\mathcal{O}(a^2/r^2, \epsilon)$—which gives a physical interpretation of the possible physical processes near the rotating non-Kerr compact object—they take the following form:

$$E^{\hat{r}} \to \frac{aBM}{r^3}\left[\cos^2\theta - 3 + 3\left(\frac{M^2}{r^2} - \frac{2M^3}{r^3} + \frac{M^3}{r^3}\sin^2\theta\right)\epsilon\right], \quad (15)$$

$$E^{\hat{\theta}} \to \frac{aBM}{r}\frac{2r^3 + \epsilon M^3}{r^3\sqrt{r^2 - 2Mr}}\sin 2\theta, \quad (16)$$

$$B^{\hat{r}} \to B\cos\theta\left[1 + \frac{a^2}{r^2}\left(1 - \frac{2M}{r}\right)\left(1 + \frac{\epsilon M^3}{r^3}\right)\right.$$
$$\left. - \frac{a^2M}{r^3}\left(2 + \frac{\epsilon M^2}{r^2} + \frac{2\epsilon M^3}{r^3}\right)\cos 2\theta\right], \quad (17)$$

$$B^{\hat{\theta}} \to B\sin\theta\left[1 + \frac{2a^2M}{r^3}\left(1 + \frac{4\epsilon M^3}{r^3}\right)\right.$$
$$\left. - \frac{a^2M}{2r^3}\left(2 + \frac{8\epsilon M^3}{r^3} + \frac{3\epsilon M^2}{r^2}\right)\sin^2\theta\right]. \quad (18)$$

In the limit of flat spacetime, i.e., for $M/r \to 0$, expressions (7)–(10) give

$$E^{\hat{r}} = E^{\hat{\theta}} \to 0, \quad (19)$$

$$B^{\hat{r}} \to B\cos\theta, \qquad B^{\hat{\theta}} \to B\sin\theta. \quad (20)$$

As expected, expressions (19) and (20) coincide with the solutions for the homogeneous magnetic field in the Newtonian spacetime.

III. THE MOTION OF CHARGED PARTICLES AROUND A ROTATING BLACK HOLE

We now study in detail the motion of charged particles around a rotating non-Kerr black hole immersed in a uniform magnetic field given by the four-vector potential (4), with the aim of testing modified gravity theories.

Hereafter we will take into account the fact that the induced electric charge of the compact object will be rapidly neutralized due to the process of selective accretion of charges from the surrounding plasma. We shall study the motion of the charged test particles around a rotating non-Kerr black hole using the Hamilton-Jacobi equation,

$$g^{\mu\nu}\left(\frac{\partial S}{\partial x^{\mu}}+eA_{\mu}\right)\left(\frac{\partial S}{\partial x^{\nu}}+eA_{\nu}\right)=-m^{2}, \tag{21}$$

where e and m are the charge and the mass of a test particle, respectively. Since t and φ are the Killing variables one can write the action in the form

$$S=-\mathcal{E}t+\mathcal{L}\varphi+S_{r\theta}(r,\theta), \tag{22}$$

where the conserved quantities $\mathcal{E}$ and $\mathcal{L}$ are the energy and the angular momentum of a test particle at infinity. By substituting this into Eq. (21) one can get the equation for the inseparable part of the action.

One can easily separate variables in this equation in the equatorial plane, $\theta=\pi/2$, and obtain the equation for radial motion,

$$\left(\frac{d\rho}{ds}\right)^{2}=\mathcal{E}^{2}-1-2V_{\text{eff}}^{2}, \tag{23}$$

where s is the proper time along the trajectory of a particle, $\rho=r/M$, and

$$\begin{aligned}V_{\text{eff}}^{2}=&\frac{1}{8\rho^{6}(\rho^{3}+\epsilon)^{2}}[16a\mathcal{E}\mathcal{L}\rho^{6}(\rho^{3}+\epsilon)+a^{4}b^{2}(2+\rho)(\rho^{3}+\epsilon)^{3}\\&+\rho^{6}\{\rho^{5}(b^{2}(\rho-2)\rho^{2}-8)+\rho^{2}\{\rho(8\mathcal{E}^{2}-4+b^{2}(\rho-2)\rho)-8\}\epsilon+4(\mathcal{E}^{2}-1)\epsilon^{2}\\&+4\mathcal{L}(\rho-2)(\rho^{3}+\epsilon)(b\rho+\mathcal{L})\}+2a^{2}\rho^{4}(\rho^{3}+\epsilon)\{[2+b\{2\mathcal{L}+b(\rho^{2}-2)\}](\rho^{3}+\epsilon)-2\mathcal{E}^{2}\rho^{2}(2+\rho)\}]\end{aligned} \tag{24}$$

can be interpreted as an effective potential of the radial motion, where $b=eBM/m$ is the magnetic parameter.

In Fig. 1 the radial dependence of the effective potential for the radial motion of charged particles in the equatorial plane of a rotating non-Kerr black hole immersed in a magnetic field is shown for the different values of the magnetic parameter, deformation parameter, and angular momentum of the black hole. From this dependence one

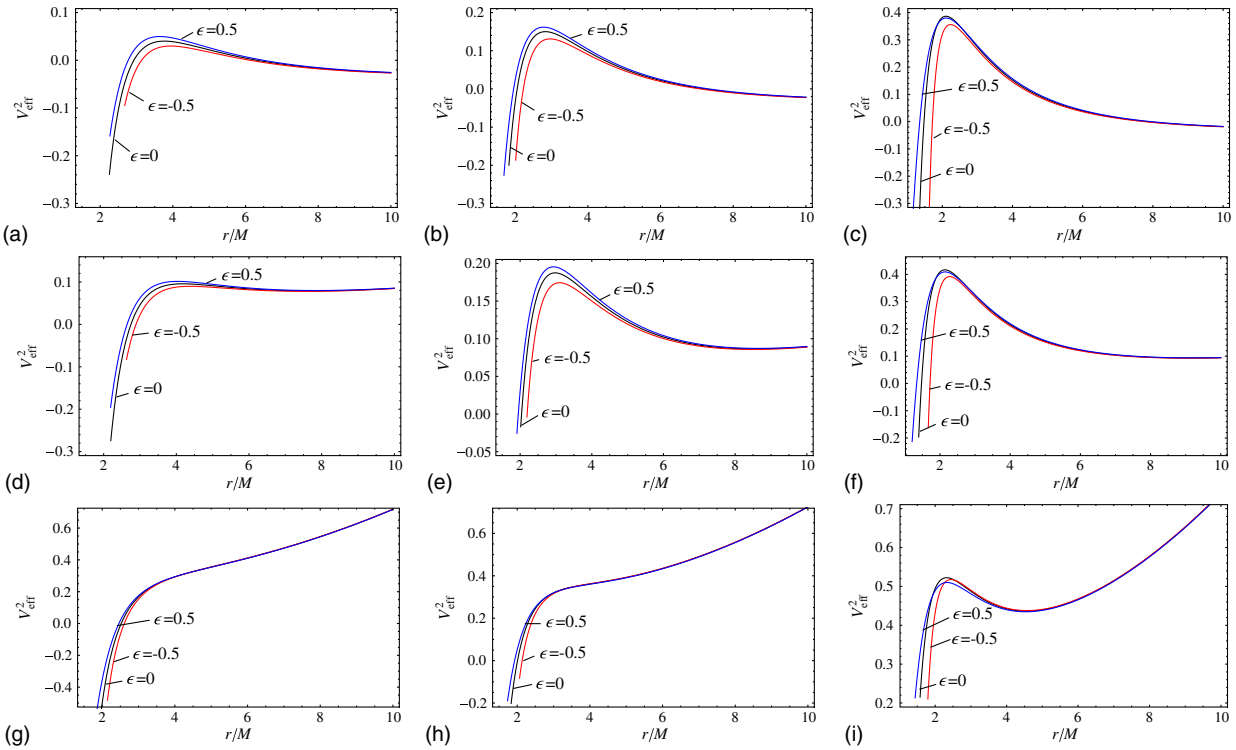

FIG. 1 (color online). The radial dependence of the effective potential of the radial motion of a charged particle around a rotating non-Kerr black hole's equatorial plane. The figures (a), (b), and (c) correspond to the case of $a=0$. The figures (d), (e), and (f) correspond to the case of $a=0.5$. The figures (g), (h), and (i) correspond to the case of $a=0.98$. The figures (a), (d), and (g) correspond to the case of $b=0$. The figures (b), (e), and (h) correspond to the case of $b=0.05$. The figures (c), (f), and (i) correspond to the case of $b=0.2$.

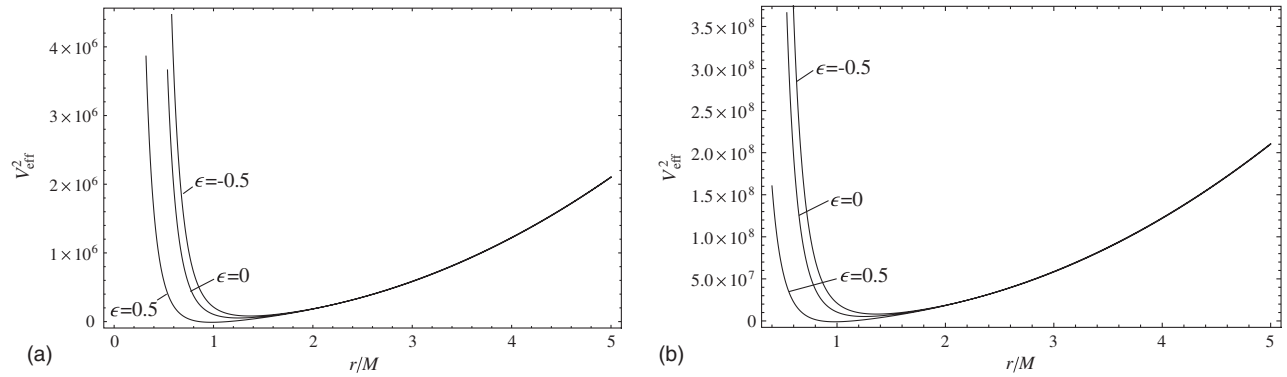

FIG. 2. The radial dependence of the effective potential of radial motion of charged particle around rotating non-Kerr black hole in equatorial plane. The figures correspond to the case of almost extreme black hole when $a = 0.99$. The figure (a) corresponds to the case when $b = 10^3$ and the figure (b) corresponds to the case when $b = 10^4$.

can obtain a modification of the radial motion of a charged particle in the equatorial plane in the presence of the deformation parameter. One can now obtain how the magnetic, rotational, and deformation parameters may change the character of the motion of the charged particles. The magnetic parameter is responsible for shifting the shape of the effective potential towards the central black hole, which means that the minimum distance of the charged particles to the central object may decrease. As is seen from the Fig. 1 the deformation parameter changes the shape of the effective potential in the vicinity of the central object. This is caused by the appearance of the new term, which proportional to the deformation parameter as $1/r^3$ in the spacetime metric tensor. When the deformation parameter is positive, $\epsilon > 0$, the shape of the effective potential shifts towards the central object, which corresponds to a decrease of the radius of the circular orbits of the test particles. The opposite effect can be observed when the deformation parameter is negative, $\epsilon < 0$: the graph shifts to the observer at infinity and corresponds to an increase of the radius of the stable orbits. With an increase of the magnetic parameter and angular momentum of the central object the minimum of the graphs shifts towards the central object. With an increase of the magnetic parameter the influence of the deformation parameter becomes weaker. Compared to the deformation parameter, the strong magnetic field dominates the behavior of the motion of the charged particles.

In a recent paper [22] it was shown that for protons and electrons the value of the dimensionless magnetic parameter is not weak, which indicates that the effect of the magnetic field on a charged particle motion is not negligible. In general such a magnetic field can essentially modify the motion of charged particles (for more details on the estimation of the magnetic parameter see, e.g., Ref. [22]). For this reason we will now study the case when the dimensionless magnetic parameter $b \gg 1$.

The radial dependence of the effective potential presented in Fig. 2 indicates the modification of the radial motion of charged particle in the equatorial plane in the presence of the strong magnetic field and the deformation parameter. As mentioned above, the magnetic parameter is responsible for the shift of the minimum distance of the charged particles towards the central object. The influence of the deformation parameter is strong in the vicinity of the central object, which is due to the strong decay of the spacetime metric tensor as $1/r^3$ with an increase of the radial coordinate. With an increase of the deformation parameter towards the positive-value side the shape of the effective potential shifts towards the central object, which corresponds to a decrease of the radius of the circular orbits of the test particles. An increase of the magnetic parameter shifts the effective potential upwards. The total energy of a test particle will increase due to the increase of the potential energy of the interaction between the magnetic field and the test charge. Compared to the deformation parameter, the strong magnetic field dominates the behavior of the motion of the charged particles.

IV. CIRCULAR ORBITS AROUND A ROTATING NON-KERR BLACK HOLE

In order to find a solution for the ISCO radius $r_{\rm ISCO}$ we assume that the external magnetic field is absent.

The expression (23) can now be written as

$$\left(\frac{d\rho}{ds}\right)^2 = f(\rho) = \frac{1}{\rho^2(\rho^3+\epsilon)}[2\rho^2(a\mathcal{E}-\mathcal{L})^2 + \rho^3(a^2\mathcal{E}^2-\mathcal{L}^2) - a^2(\rho^3+\epsilon)] + \frac{\rho^2}{(\rho^3+\epsilon)^2}[2\rho^3 + (\mathcal{E}^2-1)\rho^4 - (\rho-2)\epsilon]. \quad (25)$$

First we will consider the case when $|\epsilon| \ll 1$ in order to get an approximate analytical solution for $r_{\rm ISCO}$. Here we will take the spin parameter of the black hole as $a = 0$ in order to get the expression for the pure dependence of

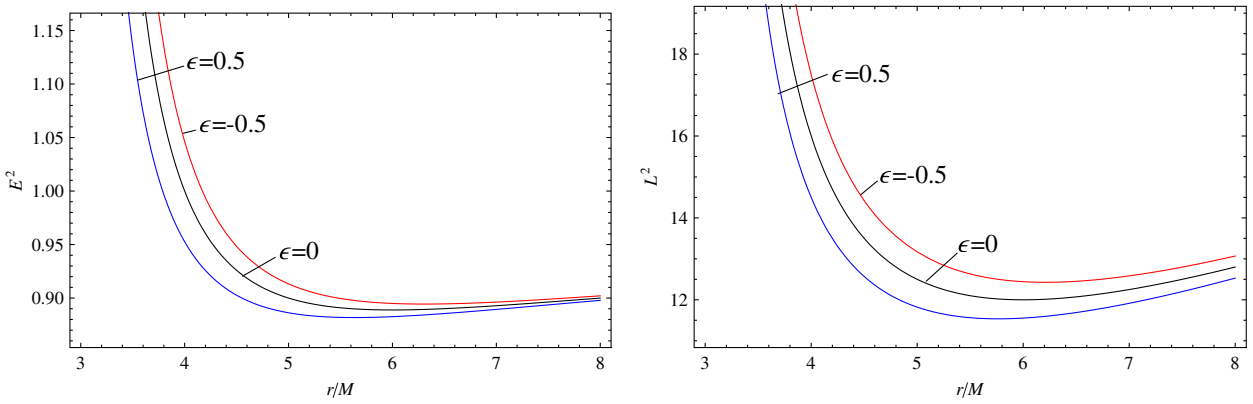

FIG. 3 (color online). Radial dependence of the energy and angular momentum of a particle moving around the rotating non-Kerr black hole on circular orbits for the different values of the deformation parameter when the dimensionless rotational parameter $a/M = 0.5$.

the ISCO radius from the deformation parameter. Using Eq. (25) and the condition of the occurrence of circular orbits $[f(r) = 0,\ f'(r) = 0]$, one can easily find expressions for the energy $\mathcal{E}$ and angular momentum $\mathcal{L}$ of a particle at a circular orbit of radius r_c, which are given as

$$\mathcal{E}^2 = \frac{(\rho-2)^2}{\rho(\rho-3)}\left(1 - \frac{\epsilon}{2\rho^2(\rho-3)}\right) + \mathcal{O}(\epsilon^2), \quad (26)$$

$$\mathcal{L}^2 = \frac{\rho^2}{\rho-3}\left(1 - \frac{3(\rho-2)^2\epsilon}{2\rho^3(\rho-3)}\right) + \mathcal{O}(\epsilon^2). \quad (27)$$

Figure 3 shows the radial dependence of both the energy and the angular momentum of a test particle moving on circular orbits around a non-Kerr black hole in the equatorial plane. One can easily see that the presence of the negative deformation parameter $\epsilon < 0$ forces a test particle to have both a larger energy and angular momentum in order to be kept in its circular orbit. This is a consequence of the increase of the gravitational potential of the rotating non-Kerr black hole with the negative deformation parameter. In the case of a positive deformation parameter, $\epsilon > 0$, the shape of the graphs shifts towards the origin, which means that the stable orbits shift towards the central object.

For the expressions (26) and (27) one can easily find a minimum radius for the circular orbits $\rho_{\rm mc} = r_{\rm mc}/M$ as

$$\rho_{\rm mc} = 3 + \frac{\epsilon}{18} + \mathcal{O}(\epsilon^2). \quad (28)$$

In the limiting case when $\epsilon = 0$, $r_{\rm mc} = 3M$, which exactly coincides with the Schwarzschild limit. The minimum radius for a stable circular orbit will occur at the point of inflexion of the function $f(\rho)$, or in other words, we must supplement the condition $f(\rho) = f'(\rho)$ with the equation $f''(\rho) = 0$. The solution in the limit of small ϵ has the following form:

$$\rho_{\rm ISCO} = 6 - \frac{2\epsilon}{9} + \mathcal{O}(\epsilon^2). \quad (29)$$

In Tables I and II we provide the numerical results for the ISCO radius of a charged particle around a rotating non-Kerr black hole immersed in an external magnetic field for different values of deformation, rotation, and magnetic parameters. From these results, one can easily get (in the case of the Schwarzschild spacetime, $a = \epsilon = b = 0$) the standard value for the ISCO radius, $\rho_{\rm ISCO} = 6M$. With an increase of the deformation parameter ϵ from -2 to 2, the radius of the ISCO as well as the relative distance from the event horizon $(r_{\rm ISCO} - r_h)/r_h$

TABLE I. The innermost stable circular orbits and the value of the expression $(r_{\rm ISCO} - r_h)/r_h$ of particles moving around the rotating non-Kerr black hole (for the case of $b = 0$).

ϵ	-2	-1	-0.5	0	0.5	1	2
$a = 0$	6.4345	6.22	6.1106	6.0	5.8884	5.776	5.5503
	2.22	2.11	2.06	2.0	1.94	1.89	1.78
$a = 0.5$	4.9286	4.5947	4.4172	4.233	4.0426	3.848	3.460
	1.58	1.43	1.35	1.27	1.18	1.09	0.90
$a = 0.7$	4.3383	3.9069	3.6625	3.3931	3.0933	2.7567	
	1.38	1.20	1.10	0.98	0.84	0.69	
$a = 0.8$	4.0604	3.5629	3.2633	2.9066	2.4431		
	1.30	1.10	0.98	0.82	0.61		
$a = 0.98$	3.6209	2.9849	2.5295	1.614			
	1.17	0.93	0.75	0.35			

TABLE II. The innermost stable circular orbits and the value of the expression $(r_{\rm ISCO} - r_h)/r_h$ of particles moving around the rotating non-Kerr black hole (for the case of $a = 0.5$).

ϵ	-2	-1	-0.5	0	0.5	1	2
$b = 0$	4.9286	4.5947	4.4172	4.233	4.0426	3.848	3.460
	1.58	1.43	1.35	1.27	1.18	1.09	0.90
$b = 0.05$	4.5857	4.3246	4.1828	4.0331	3.8758	3.7121	3.3941
	1.41	1.29	1.23	1.16	1.09	1.01	0.87
$b = 0.2$	5.6081	5.5336	3.3261	3.2377	3.1527	3.0656	
	1.94	1.93	0.77	0.74	0.70	0.66	

monotonically decrease, where the radius of the event horizon is for the equatorial plane defined from $\Delta + a^2 h = 0$ (Table I). The presence of the magnetic field also decreases the radius of the ISCO (Table II).

Now we will analyze the ISCO in the astrophysical situation where $b \gg 1$. Using the expression for the effective potential (24) and the conditions $d\rho/ds = V'_{\rm eff} = V''_{\rm eff} = 0$, one can easily find the analytic expression for the ISCO to be

$$r_{\rm ISCO} = 1 + \frac{1 - 2a^2/M^2 - \epsilon}{\sqrt{6}b} + \mathcal{O}(b^{-2}, \epsilon^2). \quad (30)$$

The relation (30) shows the qualitative dependence of the ISCO radius on both the magnetic and deformation parameters. In the limit of a strong magnetic interaction the magnetic field and the deformation parameter decrease the ISCO radius.

V. CONCLUSION

Analytic expressions for the vacuum electromagnetic fields external to a rotating non-Kerr black hole embedded in an asymptotically uniform magnetic field were presented. We derived exact expressions [Eqs. (7)–(10)] for the vacuum electromagnetic field in the vicinity of the spacetime of a rotating non-Kerr black hole, which indicate that the electromagnetic field will be affected by the deformation parameter. However, the induced electric field [Eqs. (15) and (16)] depends on the deformation parameter ϵ linearly, while the magnetic field [Eqs. (17) and (18)] depends on ϵ quadratically.

Further, the motion of charged particles around a rotating non-Kerr black hole immersed in an external uniform magnetic field have been investigated using the Hamilton-Jacobi equations of motion. We have shown that the magnetic parameter b—being responsible for the interaction between the magnetic field and he charged particles—shifts the minimum of the effective potential towards the central object, which means that the minimum distance of the charged particles to the central object decreases. The deformation parameter changes the shape of the effective potential near the central object. This is caused by the appearance of the new term, which is proportional to the deformation parameter as $1/r^3$ in the spacetime metric. When the deformation parameter is positive a decrease of the radius of the circular orbits can be observed. The opposite effect can be observed when the deformation parameter is negative, i.e., when $\epsilon < 0$ an increase of the radius of the stable orbits takes place.

We have studied in detail the influence of the magnetic, rotational, and deformation parameters on the ISCO radius of charged particles around a rotating non-Kerr black hole. An increase of the magnetic field and angular momentum of the black hole decreases the radius of the stable circular orbits. While the deformation parameter is negative the ISCO radius of the test particles becomes bigger than that for the undeformed case. For positive values of the deformation parameter the ISCO radius decreases.

The recent measurements of the ISCO radius in accretion disks around black holes may also give alternate constraints on the numerical values of the deformation parameter. All astrophysical quantities related to the observable properties of the accretion disk can be obtained from the black hole spacetime metric, and observations in the near infrared or X-ray bands have provided important information about the spin of the black holes [23]. It was stated that rotating black holes have spins in the range $0.5 \lesssim a \lesssim 1$, according to the observation that the ISCO radii are essentially shifted towards the central objects.

Because of the spacetime structure the negative deformation parameter presents some important differences with respect to the disc accretion properties when compared to the standard general relativistic Schwarzschild and Kerr ones. Therefore the study of the innermost stable orbits in the vicinity of compact objects is a powerful indicator of their physical nature. Since the ISCO radius decreases with an increase of the deformation parameter for the non-Kerr black holes, one may compare these effects with the standard general relativistic ones. Finally, since there is a correlation between the deformation parameter and the stable orbits around black holes one may numerically calculate the upper limit of the deformation parameter corresponding to the observable ISCO radius. One can put the observable values of the ISCO radius into the inequality $V''_{\rm eff}(r) < 0$ with the condition $a = 0$ and numerically solve it with respect to the deformation parameter ϵ in order to get an upper limit for the deformation parameter as $\epsilon \leq 22$.

ACKNOWLEDGMENTS

A. A. and B. A. acknowledge Akdeniz University and the TUBITAK/BIDEB Foundation for supporting local hospitality during their stay in Antalya, Turkey. A. A. and B. A. thank the TIFR and IUCAA for the warm hospitality during their stay in Mumbai and Pune, India. This research is supported in part by the projects F2-FA-F113, FE2-FA-F134, and F2-FA-F029 of the UzAS and by the ICTP through the OEA-PRJ-29 projects. A. A. and B. A. acknowledge the German Academic Exchange Service (DAAD) and the TWAS Associateship grants. B. A. thanks the ENSF, Trieste, Italy for the travel grant and the Max Planck Institute für Gravitationsphysik, Potsdam for the hospitality.

[1] W. Israel, Phys. Rev. **164**, 1776 (1967).
[2] W. Israel, Commun. Math. Phys. **8**, 245 (1968).
[3] B. Carter, Phys. Rev. Lett. **26**, 331 (1971).
[4] S. W. Hawking, Commun. Math. Phys. **25**, 152 (1972).
[5] D. C. Robinson, Phys. Rev. Lett. **34**, 905 (1975).
[6] F. Caravelli and L. Modesto, Classical Quantum Gravity **27**, 245022 (2010).
[7] T. Johannsen and D. Psaltis, Phys. Rev. D **83**, 124015 (2011).
[8] C. Bambi and L. Modesto, Phys. Lett. B **706**, 13 (2011).
[9] C. Liu, S. Chen, and J. Jing, Astrophys. J. **751**, 148 (2012).
[10] C. Bambi, F. Caravelli, and L. Modesto, Phys. Lett. B **711**, 10 (2012).
[11] S. Chen and J. Jing, Phys. Rev. D **85**, 124029 (2012).
[12] H. Krawczynski, Astrophys. J. **754**, 133 (2012).
[13] C. Bambi, Mod. Phys. Lett. A **26**, 2453 (2011).
[14] C. Bambi and E. Barausse, Phys. Rev. D **84**, 084034 (2011).
[15] M. Patil and P. S. Joshi, Phys. Rev. D **85**, 104014 (2012).
[16] A. N. Chowdhury, M. Patil, D. Malafarina, and P. S. Joshi, Phys. Rev. D **85**, 104031 (2012).
[17] V. Kagramanova, J. Kunz, and C. Laemmerzahl, Classical Quantum Gravity **25**, 105023 (2008).
[18] V. Kagramanova, J. Kunz, E. Hackmann, and C. Lammerzahl, Phys. Rev. D **81**, 124044 (2010).
[19] Z. Stuchlik and J. Schee, Classical Quantum Gravity **29**, 065002 (2012).
[20] K. Prabhu and N. Dadhich, Phys. Rev. D **81**, 024011 (2010).
[21] R. M. Wald, Phys. Rev. D **10**, 1680 (1974).
[22] V. P. Frolov and A. A. Shoom, Phys. Rev. D **82**, 084034 (2010).
[23] R. Shafee, J. E. McClintock, R. Narayan, S. W. Davis, L.-X. Li, and R. A. Remillard, Astrophys. J. **636**, L113 (2006); R. Shafee, R. Narayan, and J. E. McClintock, Astrophys. J. **676**, 549 (2008); J. F. Steiner, J. E. McClintock, R. A. Remillard, R. Narayan, and L. Gou, Astrophys. J. Lett. **701**, L83 (2009).